DEEP LEARNING ENHANCED RIS CONFIGURATION FOR URBAN SCENARIO

A PROJECT REPORT

Submitted by

ARAVINDAN S M	**2020504515**
RAMANA SRIVATS S	**2020504568**
SHRI HARISH S	**2020504583**

in partial fulfillment for the award of the degree

of

BACHELOR OF ENGINEERING

IN

ELECTRONICS AND COMMUNICATIONS ENGINEERING

DEPARTMENT OF ELECTRONICS ENGINEERING

MADRAS INSTITUTE OF TECHNOLOGY, CHROMPET

ANNA UNIVERSITY: CHENNAI 600 044

DECEMBER 2023

MADRAS INSTITUTE OF TECHNOLOGY

ANNA UNIVERSITY: CHENNAI 600 044

BONAFIDE CERTIFICATE

Certified that this project **"DEEP LEARNING ENHANCED RIS CONFIGURATION FOR URBAN SCNEARIO"**

is the bonafide work of

ARAVINDAN S M	**2020504515**
RAMANA SRIVATS S	**2020504568**
SHRI HARISH S	**2020504583**

who carried out the project work under my supervision.

SIGNATURE

Dr. P. INDUMATHI

HEAD OF THE DEPARTMENT

Professor

Department of Electronics Engineering,

Madras Institute of Technology,

Anna University

Chennai 600 044

SIGNATURE

Dr.P.PRAKASH

SUPERVISOR

Professor,

Department of Electronics Engineering,

Madras Institute of Technology,

Anna University,

Chennai – 600 044

ACKNOWLEDGEMENT

We consider it as our privilege and our primary duty to express our gratitude and respect to all those who guided and inspired us in the successful completion of the project.

We owe solemn gratitude to **Dr.J.PRAKASH**, Dean, Madras Institute of Technology, for having given consent to carry out the project work at MIT Campus, Anna University.

We wish to express our sincere appreciation and gratitude to **Dr.P.INDUMATHI**, Professor and Head of the Department of Electronics Engineering, who has encouraged and motivated us in our endeavors.

We are extremely grateful to our project guide **Dr.P.PRAKASH**, Professor, Department of Electronics Engineering, for his timely and thoughtful guidance and encouragement for the completion of the project.

We sincerely thank all our panel members **Dr. M. VASIM BABU**, Assistant Professor and **Dr. S. RAM PRABHU**, Assistant Professor of the Department of Electronics Engineering, for their valuable suggestions.

We sincerely thank our project coordinator **Dr. L. RAJESH** for her valuable suggestions. We also thank all the teaching and non-teaching staff members of the Department of Electronics Engineering for their support in all aspects.

	ARAVINDAN S M	**2020504008**
PLACE : Chennai	**RAMANA SRIVATS S**	**2020504012**
DATE :	**SHRI HARISH S**	**2020504027**

TABLE OF CONTENTS

ABSTRACT

Reconfigurable Intelligent Surfaces (RIS) play a crucial role in enhancing spectrum and energy efficiency in wireless networks. With applications ranging from enhanced Mobile BroadBand (eMBB) to Ultra-Reliable, Low-Latency Communications (URLLC) and massive Machine-Type Communications (mMTC) in 5G, their significance extends into the development of 6G systems. This study focuses on utilizing RIS for Non-Line-of-Sight (NLoS) communication. The challenge lies in optimizing a large number of RIS elements. We propose a machine learning-based model that captures the relationship between RIS phase shifts and receiver location attributes, predicting achievable rates without requiring Channel State Information (CSI) for all RIS elements. Leveraging the DeepMIMO framework, a comprehensive dataset is generated for diverse transmitter and receiver configurations. A beamforming codebook is created, and a machine learning model is trained to predict optimal RIS configurations based on receiver locations. A Feedforward Neural Network (FNN) serves as a benchmark, and a modified Convolutional Neural Network (CNN) based on AlexNet is developed for improved accuracy. Simulation results demonstrate the model's ability to recommend near-optimal RIS configurations for test receiver locations, approaching upper-bound performance assuming perfect channel knowledge. The simulation is performed at 28Ghz frequency.

.

LIST OF TABLES

LIST OF FIGURES

LIST OF ABBREVIATION

ABBREVIATION	EXPANSION
RIS	Reconfigurable Intelligent Surface
UE	User Equipment
BS	Base Station
DRL	Deep Reinforcement Learning
EM	ElectroMagnetic
DNN	Deep Neural Network
CSI	Channel State Information
OFDM	Orthogonal Frequency Division Multiplexing
CNN	Convolutional Neural Network
eMBB	enhanced mobilebroadband
mMTC	massive machinetype communications
URLC	ultra-reliable, low latency communications
SRE	Smart Radio Environment
mm-Wave	Millimeter Wave
THz	Tera Hertz
ML	Machine Learning

CHAPTER 1

INTRODUCTION

A Reconfigurable Intelligent Surface (RIS) is a novel technology that has gained significant attention in the field of wireless communications and signal processing. RIS is designed to enhance the performance of wireless communication systems by manipulating the electromagnetic waves that propagate through the environment.

1.1. 5G AND 6G OVERVIEW

In today's world, mobile wireless communication systems have become essential. But we need technology that can transmit data faster and with less delay. Mobile networks of the fifth generation (5G) and sixth generation(6G) are useful in this regard. Although they have completely changed the communication landscape, they are still in the early stages of development. 5G and 6G networks provide significantly faster data speeds compared to 4G and cuts down on latency.

Reconfigurable Intelligent Surface (RIS) has been considered as a promising technology that provides ultra-high speed for 5G beyond (5GB) and future 6G wireless communication systems. An RIS has boosted the concept of Smart Radio Environment (SRE) to enable Massive Connectivity with Massive MIMO System. RIS and Massive MIMO are both key enablers at the infrastructural level while millimeter wave (mm-Wave) and Tera Hertz (THz) communication are the key enablers at spectrum level for 5G and 6G.

1.2. SIGNIFICANCE OF LOS IN 6G

When it comes to 6G communication, the challenge is to overcome the increased signal loss and signal attenuation that comes with higher frequencies. This is due to factors such as Free-Space Path Loss, Signal attenuation increases with square of frequency, Air absorption by gases such as oxygen and water vapour, Obstructions such as foliage and rain cause additional attenuation. Electromagnetic waves at higher frequencies are more difficult to penetrate materials since Multipath propagation effects are more pronounced, Signal strength variations are common. RIS is a promising technology to overcome Line of sight (LOS) issues, since these issues are particularly common at terahertz frequency, RIS acts as an intermediary reflecting surface, Reduces LOS challenges, Optimizes signal quality, Advanced wireless communication systems such as 6G.

1.3. RECONFIGURABLE INTELLIGENT SURFACE

A Reconfigurable Intelligent Surface (RIS) is a novel technology that has gained significant attention in the field of wireless communications and signal processing. Also known as intelligent reflecting surface or intelligent reflecting environment, RIS is designed to enhance the performance of wireless communication systems by manipulating the electromagnetic waves that propagate through the environment.

The fundamental idea behind RIS involves deploying a surface made up of a large number of individually controllable elements, such as reflecting elements or antennas. RIS corresponds to a planar surface composed of a certain arrangement of unit-cells, whose properties can be dynamically controlled to change its response in the electromagnetic domain. RIS can be controlled dynamically and/or semi-statically through control signalling such to tune the incident wireless signals through reflection, refraction, focusing, collimation, modulation, absorption or any combination of these.

RIS can be implemented using mostly passive components without requiring high-cost active components such as power amplifiers, resulting in low implementation cost and energy consumption. This allows flexible deployment of RIS, with the possibility of RIS taking any shape and to be integrated onto objects (e.g. walls, buildings, lamp posts, etc.). RIS are supposed to run as nearly passive devices and hence are unlikely to increase exposure to EMF, and they can even potentially be used to reduce EM pollution in legacy deployments.

1.4. REFLECTIVE ELEMENTS

Elements that are made up of meta-atoms or unit cells play a pivotal role in shaping the behaviour of electromagnetic waves in wireless communication systems. These elements are designed to manipulate the phase, amplitude, and polarization of incident signals. They enable precise control over incident signals and their primary functions include phase manipulation for constructive interference and beamforming, amplitude modulation for signal strength adjustment, and polarization control for alignment optimization. There are two types of reflective elements.

1.4.1. PASSIVE ELEMENTS

Passive elements refer to small, reflective components that alter the properties of incoming electromagnetic waves such as polarisation, amplitude or phase rather than actively creating or amplifying signals. Since these components are usually unpowered, they don't need an external power supply. Rather, they depend on the incoming electromagnetic waves to elicit the intended outcomes. Wireless communication signal propagation can be dynamically controlled by configuring these components to intelligently focus or divert the signals.

1.4.2. ACTIVE ELEMENTS

Active elements in are specialized components embedded within the surface, equipped with the ability to actively sense the Channel State Information (CSI) of the communication channel. They are responsible for actively generating pilot signals and receiving them to estimate the channel. Active elements has 2 modes. When in the channel sensing mode, they actively gather channel information by connecting to the baseband for channel estimation and by transitioning to the reflection mode, these components use phase shifts to reflect incident signals.

1.5.OPERATING PRINCIPLES

1.5.1. ADAPTIVE CONTROL

The key feature of RIS is its ability to adaptively control the reflective elements. This adaptability is achieved through the dynamic management of reflective elements. These elements can be intelligently manipulated to respond in real-time to alterations in the wireless environment. By doing so, the RIS optimizes its configuration and behaviour, ensuring that it remains finely tuned to the prevailing communication conditions.

1.5.2. ANAMALOUS REFLECTION

A key RIS principle, anomalous reflection refers to the conversion of a wavefront from one plane wave to another. This phenomenon introduces controllable factors beyond the conventional angle of incidence and is governed by the generalised rules of reflection. In addition to the angle of incidence, other factors that affect the angles of reflection and refraction are the wavelength, refractive indices, and gradient of the phase discontinuities.

1.5.3. INTERFERENCE MITIGATION

RIS are useful instruments for mitigating interference in wireless communication networks. To increase overall signal quality and dependability, this capability entails the strategic use of the RIS to reflect or block signals. Through clever control of the reflecting components, RIS can modify the way signals propagate through the surroundings.

1.5.4. BEAM FORMING AND SIGNAL STEERING

RIS can dynamically adjust the phase and amplitude of the reflected signals, enabling precise control over signal directionality. This capability is crucial for beamforming, where signals are focused in specific directions to enhance coverage or mitigate interference.

1.5.5. CONDITION OF CO-PHASE FOR BEAMFORMING

One of the most important functions of RIS is beamforming, or focusing, especially when the system is near the source, or the terminal is close to the RIS. A crucial idea for accomplishing efficient beamforming, particularly in Line of Sight (LoS) situations, is the co-phase condition. In the co-phase condition, the RIS elements' phase shift patterns are optimised according to the observer's direction and their placements. Following this requirement enables the RIS to generate a concentrated beam that is aimed at the desired target.

1.6. MACHINE LEARNING

Machine learning, a subset of artificial intelligence (AI), is dedicated to crafting algorithms and models that empower computers to learn and make decisions or predictions autonomously, without explicit programming. This field encompasses the exploration of statistical and computational techniques that enable machines to learn and enhance their performance through experience or data. These algorithms are engineered to discern patterns and connections within data by scrutinizing and processing extensive information. Through iterative processes, machines can grasp insights from examples and accurately predict outcomes or take appropriate actions in response to new inputs. The applications of machine learning span diverse industries and domains. Some notable applications include:

Image and Speech Recognition: Machine learning methodologies have proven successful in tasks such as image classification, object detection, and speech recognition. This progress has spurred advancements in areas like autonomous vehicles, facial recognition, and voice-controlled virtual assistants.

Natural Language Processing (NLP): NLP integrates machine learning and linguistics to empower computers to comprehend, interpret, and generate human language. It finds application in sentiment analysis, language translation, and extracting information from text.

1.7. CONVOLUTIONAL NEURAL NETWORK

Neural Networks are a subset of machine learning, and they are at the heart of deep learning algorithms. They are comprised of node layers, containing an input layer, one or more hidden layers, and an output layer. Each node connects to another and has an associated weight and threshold. If the output of any individual node is above the specified threshold value, that node is activated, sending data to the next layer of the network. Otherwise, no data is passed along to the next layer of the network.

1.8. OBJECTIVE OF THE PROJECT

The aim of the research is to deploy and evaluate an innovative deep reinforcement learning framework for forecasting interaction matrices of Reconfigurable Intelligent Surfaces (RIS) in wireless communication systems. The main objective is to achieve an independent RIS operation, where the surface can arrange itself without relying on external control, thus reducing the need for beam training overhead. The evaluation will entail evaluating the framework's performance in terms of its capacity to achieve optimal convergence rates, function autonomously without external control, and efficiently minimise beam training overhead. This will ultimately enhance the practicality of RIS operation in real-world scenarios. Comparative studies will be performed by comparing against a supervised learning baseline, considering the trade-offs between the training requirements and the performance. The validation will be conducted by utilising precise 3D ray-tracing datasets in simulations, demonstrating the framework's capacity to achieve optimal rates while minimising the need for beam training overhead. This study will offer valuable information on the practical consequences and obstacles of implementing the suggested solution in actual wireless communication networks.

CHAPTER 2

LITERATURE SURVEY

Abdelrahman Taha, Muhammad Alrabeiah, and Ahmed Alkhateeb [1] (2019) worked on ‘Deep Learning for Large Intelligent Surfaces in Millimeter Wave and Massive MIMO Systems’. This paper introduces a novel approach to advancing Large Intelligent Surfaces (LISs) in beyond-5G wireless systems. The key innovation lies in a groundbreaking LIS architecture that integrates passive elements with selectively activated active elements linked to the LIS controller's baseband. This mitigates the significant training overhead associated with conventional all-passive LIS designs. The solution employs deep learning techniques, enabling the LIS to learn optimal interactions based solely on observed channels at the strategically activated elements. Simulation results demonstrate the effectiveness of this approach, achieving close proximity to theoretical upper bounds with a notable reduction in active elements. This not only enhances energy efficiency but also overcomes the training overhead challenge, making LIS systems operationally feasible.

Özgecan Özdogan, Emil Björnson[2](2020) worked on ‘Deep Learning-based Phase Reconfiguration for Intelligent Reflecting Surfaces’.This paper introduces a deep learning (DL) approach for reconfiguring the phases of Reflecting Intelligent Surfaces (RIS) in wireless communication systems. RIS, made of reconfigurable metamaterials, is a cost-effective technology that can enhance wireless communications. The configuration of RIS, particularly the local phase matrix, is challenging due to the absence of active components for pilot signal processing. The proposed DL model utilizes received pilot signals reflected through the RIS to train a deep feedforward network. Two DL methods are presented: one with a pilot length equal to the number of RIS elements and another with reduced pilot overhead. The performance is compared with a conventional least-square (LS) estimator. The results demonstrate that the DL methods outperform the LS estimator for practical pilot powers, approaching the performance of perfect channel state information. The second DL method achieves similar accuracy with reduced pilot overhead. The study suggests potential improvements, such as considering multiple users or using measured channels for DNN training.

Abdelrahman Taha, Yu Zhang, Faris B. Mismar , and Ahmed Alkhateeb [3](2020) worked on ‘Deep Reinforcement Learning for Intelligent Reflecting Surfaces: Towards Standalone Operation’. The paper addresses the challenge of configuring reflecting intelligent surfaces (RISs) efficiently without extensive training overhead. RISs play a crucial role in enhancing wireless communication by intelligently reflecting signals. The proposed solution leverages deep reinforcement learning (DRL) to enable RISs to autonomously predict optimal reflection matrices. Unlike previous supervised learning approaches, the DRL framework eliminates the need for large training datasets, making it more practical. Simulation results indicate that the DRL-based method achieves high data rates, approaching optimal performance, while requiring minimal beam training overhead. This suggests a promising direction for developing standalone and effective RIS architectures in wireless communication systems.

Mohammad Abrar Shakil Sejan, Md Habibur Rahman, Beom-Sik Shin, Ji-Hye Oh , Young-Hwan You and Hyoung-Kyu Song[4](2022) worked on ‘Machine Learning for Intelligent-Reflecting- Surface-Based Wireless Communication towards 6G: A Review’ . In this paper, a comprehensive study focusing on machine learning (ML) applications in reflecting intelligent surface (RIS) enhanced wireless communication technology. The study covers various ML-based RIS communication system model architectures, including Supervised Learning (SL), Unsupervised Learning (UL), Federated Learning (FL), and Reinforcement Learning (RL). Each model architecture is thoroughly discussed, highlighting their respective contributions and potential applications. The study concludes by outlining future research opportunities, addressing challenges, and suggesting potential applications for ML-based RIS communication. The overarching goal is to guide the efficient development and design of high-performance systems for the next generation of wireless communication. The hope is that ML-based RIS systems will significantly contribute to the advancement and optimization of wireless communication technologies in the future.

Meng Xu, Shun Zhang , Caijun Zhong[5](2021) worked on 'Ordinary Differential Equation-Based CNN for Channel Extrapolation Over RIS-Assisted Communication'.The paper introduces an innovative approach to address channel extrapolation challenges in Reconfigurable Intelligent Surface (RIS)-assisted wireless communication systems. The proposed method involves the strategic sub-sampling of RIS elements, effectively reducing the length of the pilot sequence for channel estimation. A sophisticated deep learning model is then employed, specifically an Ordinary Differential Equation (ODE)-based Convolutional Neural Network (CNN), to extrapolate complete channel information from the partial dataset. Notably, the ODE-based CNN structure exhibits superior performance in terms of faster convergence speed and more accurate solutions when compared to a conventional CNN. Through detailed simulations in an indoor communication scenario, the study convincingly illustrates the efficiency of the proposed methodology in enhancing RIS-aided communication systems.

Baoling Sheen, Jin Yang, Xianglong Feng, and Md Moin Uddin Chowdhury[6](2021) worked on ‘A Deep Learning Based Modelling of Reconfigurable Intelligent Surface Assisted Wireless Communications for Phase Shift Configuration’. This paper introduces a Machine Learning(ML)-based approach to predict optimal Reconfigurable Intelligent Surface (RIS) phase shifts in wireless communication networks. The proposed deep learning (DL) model captures interactions between the environment and the communication network, learning the mapping between RIS-embedded environments and achievable data rates at receiver locations. Notably, the model achieves near-optimal data rates using a small fraction of receiver locations and generalizes well to unseen RIS configurations. Simulation results compare favourably with baseline approaches, demonstrating the potential of ML in optimizing RIS configurations. The authors suggest future extensions to multi-user scenarios and real-world data application, emphasizing the potential synergy between ML and traditional analytical methods.

CHAPTER 3
EXISTING METHODOLOGY

3.1. ANN MODEL

The paper [1] introduces an approach for designing Reconfigurable Intelligent Surface (RIS) interaction matrices in wireless communication systems. The RIS architecture includes a small number of active elements along with passive elements, addressing the challenge of training overhead associated with massive passive components. The system operates in two phases: a learning phase and a prediction phase. In the learning phase, an exhaustive search is performed, collecting data samples for a deep learning model, specifically, an Artificial Neural Network (ANN). This ANN is implemented as a Multi-Layer Perceptron, trained to map sampled channel vectors, obtained during channel estimation, to optimal achievable rates. The prediction phase employs the trained ANN model to predict the optimal reflection beamforming vector directly from estimated sampled channels, enabling the RIS to approach near-optimal data rates with minimal training overhead and a reduced number of active elements.

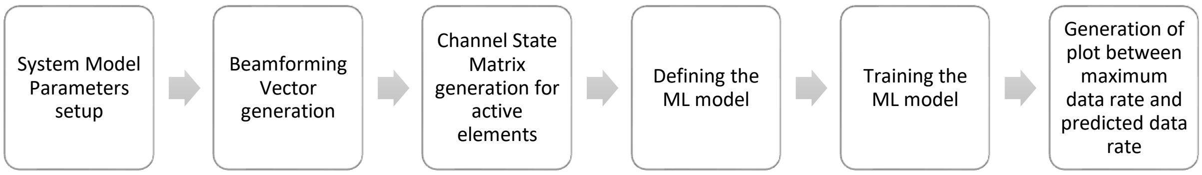

Figure 3.1 WORKFLOW

3.2. BEAMFORMING CODEBOOK

A beamforming codebook is an essential element for designing antenna arrays to broadcast or receive signals in predetermined directions. The system is comprised of a fixed collection of beamforming vectors, with each vector representing a unique beam or direction that the antenna array can concentrate its signals towards. The main purpose of a beamforming codebook is to expedite the adjustment of the antenna array to varying communication conditions, enabling the array configuration to be dynamically modified according to the environment and user positions.

The generation of a beamforming codebook entails various essential procedures. The array's beam steering is limited to specific angles, which are quantized. Quantization establishes a predetermined set of directions for the array to concentrate on. Subsequently, the analysis focuses on the geometric characteristics of the antenna array, encompassing the quantity of elements in each dimension (such as rows and columns for a two-dimensional array) and the distance between adjacent elements.

The next step entails computing the phase shifts corresponding to each quantized angle. To achieve constructive interference in the desired direction, the codebook calculates phase changes for each direction, ensuring that signals from various antenna elements align. The phase shifts act as the allocated weights for each antenna element during beam steering. The aggregation of these computed weights for all discretized angles leads to the creation of the beamforming codebook. While in operation, the beamforming system chooses a particular beamforming vector from the codebook according to the current communication scenario.

INPUT PARAMETER	DESIGNATED VALUE
Mx(Number of elements in x direction)	1
My(Number of elements in y direction)	4
Mz(Number of elements in z direction)	2
over sampling factor for x	1
over sampling factor for y	1
over sampling factor for z	1
ant_spacing(Antenna spacing)	0.5 λ

Table 3.1 INPUT PARAMETER VALUES FOR CODEBOOK

The codebook generated for the sample input parameters mentioned in table 3.1 where each row encapsulates a distinct combination of beamforming vectors within the three-dimensional space of the Uniform Planar Array (UPA). These rows represent unique spatial directions or angles in the x, y, and z dimensions, forming complete beamforming vectors for the UPA and each column signifies a specific dimension, with the first column indicating the beamforming vectors in the x-direction, the second in the y-direction, and the third in the z-direction**.** The over sampling factor interpolates or multiplies the sampling rate by the given number. Oversampling involves sampling a signal at a rate higher than the minimum required rate, and it is commonly used in signal processing to provide additional information about the signal. In the context of beamforming codebook generation, oversampling is employed to improve the granularity of the codebook, allowing for more fine-tuned adjustments in the direction of beamforming.

3.3. CHANNEL GENERATION BETWEEN TRANSMITTER AND RECEIVER THROUGH RIS

The DeepMIMO library provides a comprehensive solution for generating and simulating wireless communication channels, specifically designed for urban environments. This multifunctional application enables users to specify and simulate intricate ray tracing scenarios that involve a transmitter, receiver, and Reconfigurable Intelligent Surface (RIS). By providing crucial parameters, users can acquire useful information regarding the simulated scenario.

Channel Matrix:

During simulation, the library grants access to the channel matrix, a vital element for comprehending the attributes of the wireless communication channel. The channel matrix represents the connection between the signals that are transmitted and the signals that are received, taking into account the influence of reflections, diffractions, and other factors related to signal propagation.

Distance between Transmitter (Tx) and Receiver (Rx):

Another important result obtained from the simulation is the measurement of the distance between the transmitter (Tx) and receiver (Rx). This value is crucial for evaluating the propagation properties of wireless signals and comprehending the spatial correlation between the communicating entities.

The DeepMIMO library provides users with comprehensive outputs, enabling them to analyse and optimise wireless communication systems in urban contexts. It considers the complex interactions between elements and propagation phenomena. Gaining insights into channel characteristics, ray tracing, and spatial linkages improves comprehension of real-life communication scenarios and assists in the development and assessment of wireless networks.

Parameters	Value
Scenario	28GHz (01_28)
Dynamic Setting	First Scene:1, Last Scene:1
Number of Paths	1
First User Row	850
Row Subsampling	1
User Subsampling	1
Enable BS2BS (Base Station to Base Station)	True
OFDM channels	1
OFDM Subcarriers	512
OFDM Subcarriers limit	64
OFDM bandwidth	0.1

Table 3.2 TRANSMITTER TO RIS SAMPLE PARAMETERS

Parameters	Value
Scenario	28GHz (01_28)
Dynamic Setting	First Scene:1, Last Scene:1
Number of Paths	1
First User Row	1000
Last User Row	1300
Row Subsampling	1
User Subsampling	1
Enable BS2BS (Base Station to Base Station)	True
OFDM channels	1
OFDM Subcarriers	512
OFDM Subcarriers limit	64
OFDM bandwidth	0.1

Table 3.3 RECEIVER TO RIS SAMPLE PARAMETERS

The simulation setup involves several input parameters. The 'dataset_folder' parameter designates the directory path for loading the dataset. The 'scenario' parameter defines the scenario configuration, such as '01_28' indicating a scenario operating at 28 GHz. The 'dynamic_settings' dictionary includes settings related to dynamic aspects, specifying the starting and last scenes. Other parameters include 'num_paths' for the number of paths from the transmitter to RIS element, 'active_BS' as a NumPy array indicating active base stations, and 'user_row_first'/'user_row_last' determining the range of rows for user locations. Additional details involve 'bs_antenna' and 'ue_antenna' dictionaries describing base station and user equipment antennas, respectively. 'enable BS2BS' is set to 1, enabling base station-to-base station communication. The 'OFDM_channels' parameter signifies the number of OFDM channels, set to 1. The 'OFDM' dictionary within includes subcarrier-related details such as the number, sampling, and bandwidth.

3.4. DEEPMIMO DATASET

The DeepMIMO dataset is used in this project to simulate the scenario of a wireless channel with RIS. DeepMIMO is a generic dataset for mmWave/massive MIMO channels. The DeepMIMO dataset generation framework has two important features. First, the DeepMIMO channels are constructed based on accurate ray-tracing data obtained from Remcom Wireless InSite. The DeepMIMO channels, therefore, capture the dependence on the environment geometry/materials and transmitter/receiver locations, which is essential for several machine learning applications. Second, the DeepMIMO dataset is generic/parameterized as the researcher can adjust a set of system and channel parameters to tailor the generated DeepMIMO dataset for the target machine learning application.

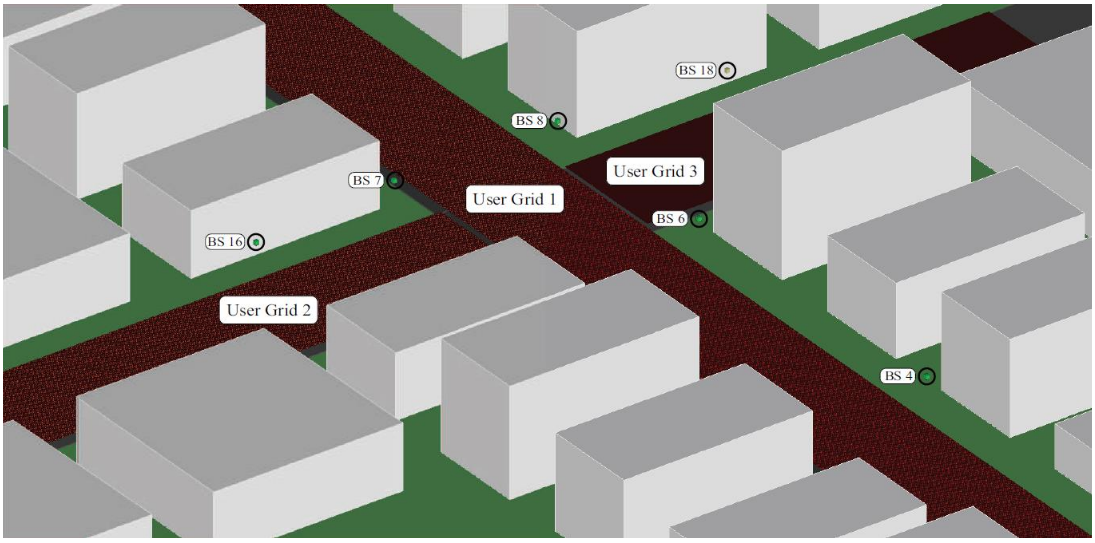

Figure 3.2 BIRD EYE VIEW OF THE 28 GHz URBAN SCENARIO

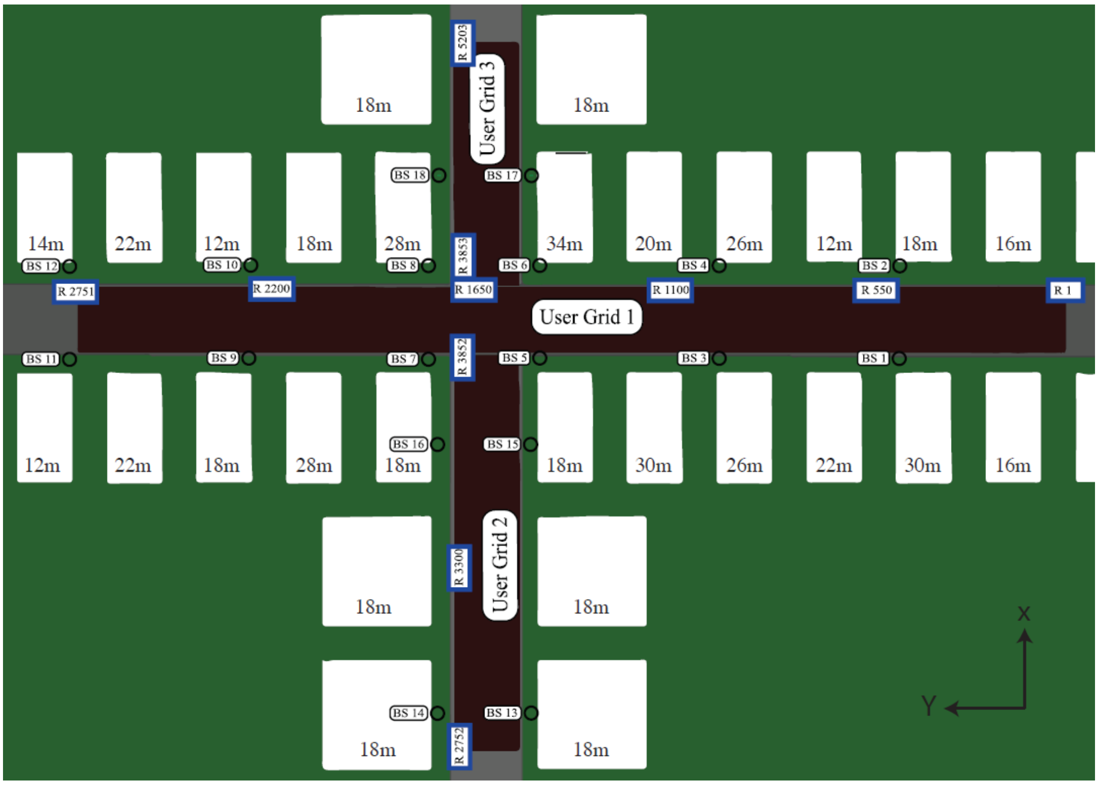

Figure 3.3 TOP VIEW OF 28 GHz URBAN SCENARIO

Figures 3.5 and 3.6 represents an urban scenario operating at 28GHz . It is a MATLAB 3d urban model with n number of base stations and antenna array where we can simulate a wireless communication link by setting the required parameters.

3.5. FEEDFORWARD NEURAL NETWORK

A feedforward neural network is a basic and straightforward sort of artificial neural network. Within this network, information only flows in a unidirectional manner, progressing from the input nodes, passing via any hidden nodes, and ultimately reaching the output nodes. The network is acyclic. Feedforward neural networks were the initial form of artificial neural networks developed and are less complex compared to other types such as recurrent neural networks and convolutional neural networks.

Natural Language Processing (NLP) is the field of study that focuses on the interaction between computers and human language. It involves developing algorithms and models to enable computers to understand, interpret, and generate human language in a way that is both accurate and meaningful. Natural Language Processing (NLP) combines machine learning and linguistics to enable computers to understand, interpret, and produce human language. It is utilized in sentiment analysis, language translation, and text information extraction. A feedforward neural network is composed of three distinct layers: the input layer, hidden layers, and the output layer. Each layer consists of neurons, and the layers are connected by weights.

The input layer comprises neurons that accept inputs and transmit them to the subsequent layer. The quantity of neurons in the input layer is dictated by the dimensions of the input data.

Hidden layers are unexposed to the input or output and can be regarded as the computational core of the neural network. The neurons in each hidden layer calculate the weighted sum of the outputs from the previous layer, apply an activation function to it, and transmit the resulting value to the next layer. The network may possess zero or several hidden levels.

Output Layer: The ultimate layer responsible for generating the output based on the provided inputs. The quantity of neurons in the output layer is contingent upon the total number of potential outputs that the network is intended to generate.

3.6. MODEL DEFINITION AND LAYOUT

The model defined is a type of feedforward neural network, specifically a fully connected or dense neural network. It consists of a sequence of fully connected layers with ReLU activations and dropout layers. The architecture follows a feedforward design where each neuron in one layer is connected to every neuron in the next layer.

The specific architecture is as follows:

Input Layer:

A single input layer (imageInputLayer) with the specified size. This layer is responsible for ingesting the input data into the network.

Hidden Layers:

The core of the neural network consists of three sets of hidden layers. Each hidden layer is implemented using fullyConnectedLayer. Each hidden layer is followed by a Rectified Linear Unit (ReLU) activation function. Additionally, dropout layers are inserted after each fully connected layer.

Output Layer:

A fully connected layer (fullyConnectedLayer) with a regression layer (regressionLayer) for regression tasks.

3.7.ANN MODEL ANALYSIS

The ANN model has been implemented and the analysis is given by

ANALYSIS RESULT

	Name	Type	Activations	Learnable Proper...	States
1	input 768×1×1 images with 'zerocenter' norma...	Image Input	768(S) × 1(S) × 1(C) × 1(B)	-	-
2	Fully1 144 fully connected layer	Fully Connected	1(S) × 1(S) × 144(C) × 1(B)	Weights 144 × 768 Bias 144 × 1	-
3	relu1 ReLU	ReLU	1(S) × 1(S) × 144(C) × 1(B)	-	-
4	dropout1 50% dropout	Dropout	1(S) × 1(S) × 144(C) × 1(B)	-	-
5	Fully2 576 fully connected layer	Fully Connected	1(S) × 1(S) × 576(C) × 1(B)	Weights 576 × 144 Bias 576 × 1	-
6	relu2 ReLU	ReLU	1(S) × 1(S) × 576(C) × 1(B)	-	-
7	dropout2 50% dropout	Dropout	1(S) × 1(S) × 576(C) × 1(B)	-	-
8	Fully3 576 fully connected layer	Fully Connected	1(S) × 1(S) × 576(C) × 1(B)	Weights 576 × 576 Bias 576 × 1	-
9	relu3 ReLU	ReLU	1(S) × 1(S) × 576(C) × 1(B)	-	-
10	dropout3 50% dropout	Dropout	1(S) × 1(S) × 576(C) × 1(B)	-	-
11	Fully4 144 fully connected layer	Fully Connected	1(S) × 1(S) × 144(C) × 1(B)	Weights 144 × 576 Bias 144 × 1	-
12	outReg mean-squared-error	Regression Output	1(S) × 1(S) × 144(C) × 1(B)	-	-

Figure 3.4 ANN MODEL LAYERS

Fig.3.7 shows the layers used in ANN model for simulation. The subsequent columns give us the information about the type of layer and the dimensions of the inputs and their respective weights and bias.

CHAPTER 4

PROPOSED METHODOLOGY

4.1. ALEXNET MODEL SUMMARY

The proposed methodology introduces a novel approach to Reconfigurable Intelligent Surface (RIS) design for wireless communication systems, aiming to optimize interaction matrices. In contrast to the ANN model, the proposed approach integrates an AlexNet model, a Convolutional Neural Network (CNN), in place of the Artificial Neural Network (ANN) for machine learning tasks. The two-phase system comprises a learning phase and a prediction phase. During the learning phase, an exhaustive search is conducted to collect data samples for training the AlexNet model. The AlexNet, known for its effectiveness in image classification tasks, is adapted to map sampled channel vectors obtained during channel estimation to optimal achievable rates.

In the prediction phase, the trained AlexNet model is utilized to predict the optimal reflection beamforming vector directly from estimated channel samples. This integration of a CNN facilitates improved feature extraction and abstraction, potentially enhancing the system's ability to capture intricate patterns within the data. The proposed methodology aims to leverage the capabilities of deep learning models, specifically AlexNet, to achieve near-optimal data rates for RIS-enabled communication systems while mitigating training overhead associated with extensive search algorithms. Extensive simulations are conducted to validate the efficacy of the proposed AlexNet-based methodology, showcasing its potential advantages over traditional ANN-based approaches.

4.2. ALEXNET MODEL

AlexNet is a convolutional neural network (CNN) architecture that played a crucial role in advancing the field of computer vision and deep learning. It was developed by Alex Krizhevsky, Ilya Sutskever, and Geoffrey Hinton, and it won the ImageNet Large Scale Visual Recognition Challenge (ILSVRC) in 2012. The architecture of AlexNet demonstrated the effectiveness of deep learning in image classification tasks.

4.3. ALEXNET ARCHITECTURE

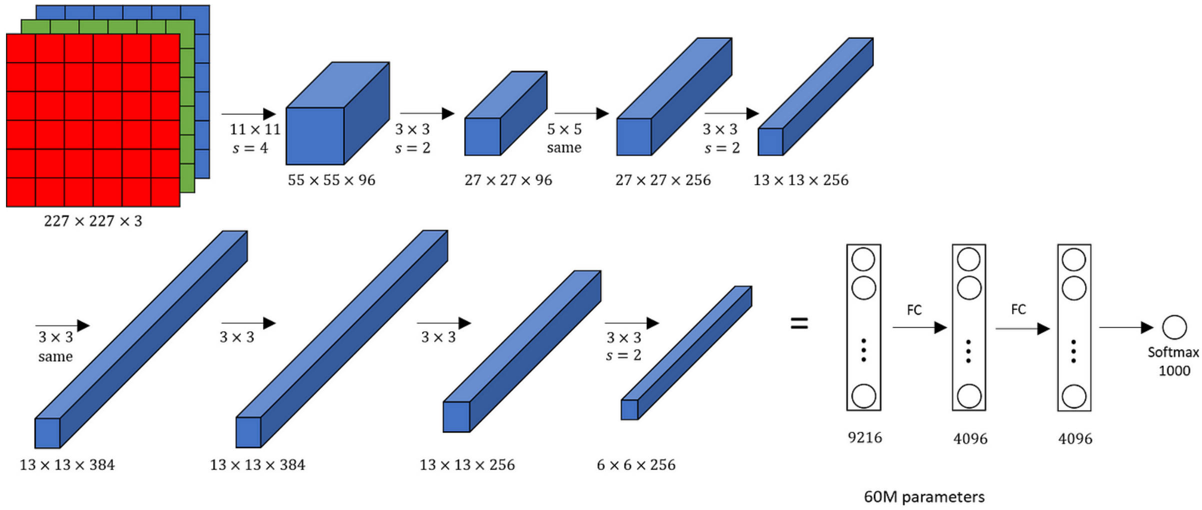

Figure 4.1 ALEXNET LAYER ARCHITECTURE

The AlexNet contains 8 layers with weights;

5 convolutional layers

3 fully connected layers.

At the end of each layer, ReLu activation is performed except for the last one, which outputs with a softmax with a distribution over the 1000 class labels. Dropout is applied in the first two fully connected layers. As the figure above shows also applies Max-pooling after the first, second, and fifth convolutional layers. The kernels of the second, fourth, and fifth convolutional layers are connected only to those kernel maps in the previous layer, which reside on the same GPU. The kernels of the third convolutional layer are connected to all kernel maps in the second layer. The neurons in the fully connected layers are connected to all neurons in the previous layer.

4.3.1. CONVOLUTIONAL LAYER

The convolutional layer is considered an essential block of the CNN. In a CNN, it is crucial to understand that the layers' parameters and channel are comprised of a set of learnable channels or neurons. These channels have a small receptive field. In the feed forward process, every individual channel goes over the dimensions of the input, thus calculating the dot product from the filter (kernel) pixels and the input pixels. The result of this calculation is a two-dimensional feature map. Through this, the system learns channels made when it detects some specific sort of feature at a spatial location within the feature map. Every one of the neurons calculates convolutions with small portions , as shown in Eq.

$$y_i = b_i + \sum_{x_i \in x} W_{\mathrm{ij}} * x_i \tag{4.1}$$

Where yi ∈ Y, i = 1,2,…D. D is the depth of the convolutional layer. Each filter Wij is a 3D matrix of size [F × F × CX]. Its size is determined by a selected receptive field (F), and its feature-map input's depth (CX). An individual neuron in the next layer is associated with certain neurons in the previous layer, called the receptive field. The local region features from the input matrix are extracted utilizing a receptive field. A neuron's receptive field is related to a specific portion in the previous layer and frames a weight vector.

4.3.2. FULLY CONNECTED LAYER

A Fully Connected Layer, also known as a dense layer, is a type of layer in a neural network where each neuron or node in the layer is connected to every neuron in the preceding layer. In other words, each neuron in a fully connected layer receives input from every output of the previous layer. These connections are often associated with learnable parameters, including weights and biases.

Connectivity:

Every neuron in a fully connected layer is connected to every neuron in the previous layer. This results in a dense and fully connected structure, as opposed to other layer types, such as convolutional layers, which have local connectivity.

Learnable Parameters:

The connections between neurons in a fully connected layer are associated with learnable parameters, namely weights and biases. Each connection has a weight that determines the strength of the connection, and each neuron has a bias term.

Input and Output:

The input to a fully connected layer is the output from the preceding layer. If the preceding layer has N neurons, then each neuron in the fully connected layer receives N inputs. The output of each neuron is computed based on a weighted sum of these inputs, and an activation function may be applied to introduce non-linearity.

Parameters and Complexity:

The number of parameters in a fully connected layer can be substantial, especially in networks with a large number of neurons. This can contribute to increased computational complexity and potential overfitting, especially if the network has limited training data.

Activation Function:

An activation function is typically applied to the output of each neuron in a fully connected layer to introduce non-linearity. Common activation functions include Rectified Linear Unit (ReLU), sigmoid, or hyperbolic tangent (tanh).

Output Size:

The number of neurons in the fully connected layer determines the size of the output. In classification tasks, the number of neurons in the final fully connected layer corresponds to the number of classes.

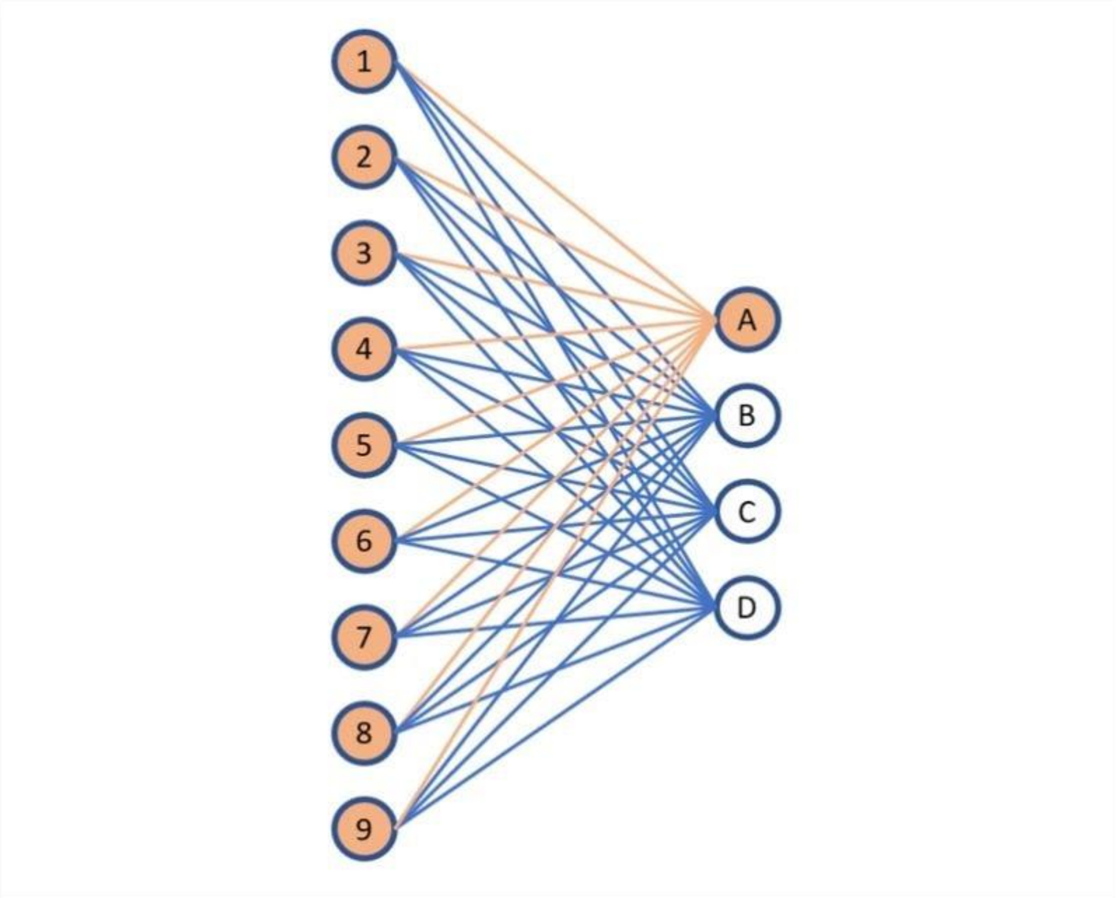

Figure 4.2 FULLY CONNECTED LAYER STRUCTURE

Fig.4.2 shows a diagrammatic representation of a fully connected layer in machine learning models.

4.3.3. DROPOUT LAYER

Usually, when all the features are connected to the FC layer, it can cause overfitting in the training dataset. Overfitting occurs when a particular model works so well on the training data causing a negative impact in the model's performance when used on new data. To overcome this problem, a dropout layer is utilized 8 wherein a few neurons are dropped from the neural network during the training process resulting in reduced size of the model. On passing a dropout of 0.3, 30% of the nodes are dropped out randomly from the neural network. Dropout results in improving the performance of a machine learning model as it prevents overfitting by making the network simpler. It drops neurons from the neural networks during training.

4.3.4. POOLING LAYER

In most cases, a Convolutional Layer is followed by a Pooling Layer. The primary aim of this layer is to decrease the size of the convolved feature map to reduce the computational costs. This is performed by decreasing the connections between layers and independently operates on each feature map. In Max Pooling, the largest element is taken from the feature map. Average Pooling calculates the average of the elements in a predefined size Image section. The total sum of the elements in the predefined section is computed in Sum Pooling. The Pooling Layer usually serves as a bridge between the Convolutional Layer and the Fully Connected Layer. The CNN model generalizes the features extracted by the convolution layer and helps the networks to recognize the features independently. With the help of this, the computations are also reduced in a network.

4.3.5. RELU ACTIVATION FUNCTION

ReLU, which stands for Rectified Linear Unit, is an activation function commonly used in neural networks, particularly in deep learning models. It introduces non-linearity to the network, allowing it to learn complex patterns in the data. The ReLU activation function is defined mathematically as:

$$f(x)=\max(0,x) \tag{4.2}$$

In simple terms, the output of the ReLU function is the maximum of zero and the input x. The function is linear for positive input values and zero for negative input values. Visually, the ReLU activation function looks like a piecewise linear function with a threshold at zero.

4.4. ALEXNET MODEL DEFINITION

This model begins with an input layer (imageInputLayer) designed for a specific input size of [768,1,1]. The subsequent layers Transfer block incorporates modified AlexNet layers (from layers 2 to 10), which include pooling layers (pool1_mod, pool2_mod) and convolutional layers (conv1_mod, conv2_mod, conv3_mod). These layers are adjusted with considerations such as filter size, number of filters, and stride. The modified layers replace the corresponding layers in the original AlexNet. After the convolutional layers, the model integrates fully connected layers (fc6, fc7, fc8, fc9) with ReLU activations (relu6, relu7, relu8) and dropout layers (drop6, drop7, drop8) for improved generalization. The output is a regression layer (regLayer) for tasks involving continuous value prediction.

4.5. ALEXNET BASED CNN MODEL ANALYSIS

ANALYSIS RESULT

	Name	Type	Activations	Learnable Proper...	States
1	inputLayer 768x1x1 images	Image Input	768(S) × 1(S) × 1(C) × 1(B)	-	-
2	conv1_mod 96 3x3 convolutions with stride [1 1] and ...	2-D Convolution	768(S) × 1(S) × 96(C) × 1(B)	Weig... 3 × 3 × 1 ... Bias 1 × 1 × 96	-
3	relu1 ReLU	ReLU	768(S) × 1(S) × 96(C) × 1(B)	-	-
4	norm1 cross channel normalization with 5 chann...	Cross Channel Norm...	768(S) × 1(S) × 96(C) × 1(B)	-	-
5	pool1_mod 2x2 max pooling with stride [2 2] and pa...	2-D Max Pooling	385(S) × 1(S) × 96(C) × 1(B)	-	-
6	conv2_mod 2 groups of 128 3x3 convolutions with st...	2-D Grouped Convo...	385(S) × 1(S) × 256(C) × 1(B)	Wei... 3 × 3 × 48 ... Bias 1 × 1 × 128...	-
7	relu2 ReLU	ReLU	385(S) × 1(S) × 256(C) × 1(B)	-	-
8	norm2 cross channel normalization with 5 chann...	Cross Channel Norm...	385(S) × 1(S) × 256(C) × 1(B)	-	-
9	pool2_mod 2x2 max pooling with stride [2 2] and pa...	2-D Max Pooling	193(S) × 1(S) × 256(C) × 1(B)	-	-
10	conv3_mod 384 3x3 convolutions with stride [1 1] an...	2-D Convolution	193(S) × 1(S) × 384(C) × 1(B)	Wei... 3 × 3 × 256... Bias 1 × 1 × 384	-
11	fc6 2304 fully connected layer	Fully Connected	1(S) × 1(S) × 2304(C) × 1(B)	Weigh... 2304 × 74... Bias 2304 × 1	-
12	relu6 ReLU	ReLU	1(S) × 1(S) × 2304(C) × 1(B)	-	-
13	drop6 50% dropout	Dropout	1(S) × 1(S) × 2304(C) × 1(B)	-	-
14	fc7 1152 fully connected layer	Fully Connected	1(S) × 1(S) × 1152(C) × 1(B)	Weigh... 1152 × 23... Bias 1152 × 1	-
15	relu7 ReLU	ReLU	1(S) × 1(S) × 1152(C) × 1(B)	-	-
16	drop7 50% dropout	Dropout	1(S) × 1(S) × 1152(C) × 1(B)	-	-
17	fc8 576 fully connected layer	Fully Connected	1(S) × 1(S) × 576(C) × 1(B)	Weights 576 × 1152 Bias 576 × 1	-
18	relu8 ReLU	ReLU	1(S) × 1(S) × 576(C) × 1(B)	-	-
19	drop8 50% dropout	Dropout	1(S) × 1(S) × 576(C) × 1(B)	-	-
20	fc9 144 fully connected layer	Fully Connected	1(S) × 1(S) × 144(C) × 1(B)	Weights 144 × 576 Bias 144 × 1	-
21	reg mean-squared-error	Regression Output	1(S) × 1(S) × 144(C) × 1(B)	-	-

Figure 4.3 MODIFIED ALEXNET MODEL LAYERS

Fig.4.4 shows the different layers used in the Alexnet model. The neural network architecture starts with an imageInputLayer with dimensions [768, 1, 1], which acts as the input layer for a particular image size. The convolutional layers, ReLU activation layers, and pooling layers from the pre-trained AlexNet are transferred to layers 2 to 10. The following layers undergo alterations, beginning with pool1_mod, which is a maxPooling2dLayer with a pool size of 2x2, 2 strides, and padding of 1. Next, conv1_mod is a convolution2dLayer that utilises a 3x3 filter size, 96 filters, a stride of 1, and a padding of 1. Conv2_mod is a groupedConvolution2dLayer with a filter size of 3x3, 128 filters, separated into 2 groups, and has the same stride and padding. Pool2_mod is an altered version of the maxPooling2dLayer, and conv3_mod is the subsequent layer, which is a convolution2dLayer with a filter size of 3x3 and 384 filters.

The network architecture includes an extra layer called fc6, which is a fully connected layer with a number of neurons determined by multiplying the outSize by 16. This is followed by a reluLayer (relu6) and a dropoutLayer (drop6) with a dropout rate of 0.5. Following that, a fullyConnectedLayer called fc7 is implemented, with the number of neurons determined by multiplying the outSize by 8. This is then followed by relu7 and drop7 layers. The architectural sequence proceeds with fc8, a fullyConnectedLayer including a quantity of neurons determined by multiplying outSize by 4. This is thereafter followed by relu8 and drop8 layers. The fc9 layer is a fully connected layer that has a specific number of neurons determined by the outSize parameter. The architecture of the network is completed with a regression layer, also known as regLayer.

Additional improvements to the architecture involve the addition of a dropout layer (drop9) as the 19th layer, which introduces regularisation with a dropout rate of 0.5. The 20th layer is a fullyConnectedLayer (fc10) consisting of 144 neurons, which is a customised configuration. The 21st layer is a regression Layer called reg Output. It calculates the mean squared error, which quantifies the discrepancy between the predicted and actual results. The mentioned additions enhance the complexity of the network by introducing regularisation to enhance generalisation and a specialised fully linked layer. The regression output layer, which utilises mean squared error calculation, functions as the ultimate stage for evaluating the model's performance.

CHAPTER 5
RESULTS AND DISCUSSION

5.1. CODEBOOK GENERATION OF BEAM FROMING VECTORS

```
                     0                    1                    2  \
0  0.353553+0.000000j   0.353553+0.000000j   0.353553+0.000000j
1  0.332232-0.120922j   0.006170+0.353500j  -0.336249-0.109254j
2  0.270838-0.227260j  -0.353338+0.012339j   0.286031+0.207813j
3  0.176777-0.306186j  -0.018504-0.353069j  -0.207814-0.286030j
4 -0.353553-0.000000j  -0.353553-0.000000j  -0.353553-0.000000j
5 -0.332232+0.120922j  -0.006170-0.353500j   0.336249+0.109254j
6 -0.270838+0.227260j   0.353338-0.012339j  -0.286031-0.207813j
7 -0.176777+0.306186j   0.018504+0.353069j   0.207814+0.286030j

                     3                    4                    5  \
0  0.353553+0.000000j   0.353553+0.000000j   0.353553+0.000000j
1  0.212773-0.282361j   0.332232-0.120922j   0.006170+0.353500j
2 -0.097453-0.339857j   0.270838-0.227260j  -0.353338+0.012339j
3 -0.330071-0.126701j   0.176777-0.306186j  -0.018504-0.353069j
4 -0.353553-0.000000j  -0.353553+0.000000j  -0.353553+0.000000j
5 -0.212773+0.282361j  -0.332232+0.120922j  -0.006170-0.353500j
6  0.097453+0.339857j  -0.270838+0.227260j   0.353338-0.012339j
7  0.330071+0.126701j  -0.176777+0.306186j   0.018504+0.353069j

                     6                    7
0  0.353553+0.000000j   0.353553+0.000000j
1 -0.336249-0.109254j   0.212773-0.282361j
2  0.286031+0.207813j  -0.097453-0.339857j
3 -0.207814-0.286030j  -0.330071-0.126701j
4 -0.353553+0.000000j  -0.353553+0.000000j
5  0.336249+0.109254j  -0.212773+0.282361j
6 -0.286031-0.207813j   0.097453+0.339857j
7  0.207814+0.286030j   0.330071+0.126701j
```

Figure 5.1 BEAM FORMING VECTORS FOR SAMPLE PARAMETERS

The above fig.5.1 depicts all possible beam forming vector configurations of RIS for given dimensions and parameters of RIS. The ML model chooses the best beamforming vector from this codebook to get maximum data rate. For each configuration from the code book RIS will form beams in different direction. For a given receiver location one beam forming vector from the codebook will give maximum data rate. The above output is obtained for a 8*8 RIS . The complex numbers represent the beamforming vectors and each row represent the various beam steering angles for the corresponding RIS element.

5.2. ANN MODEL RESULTS

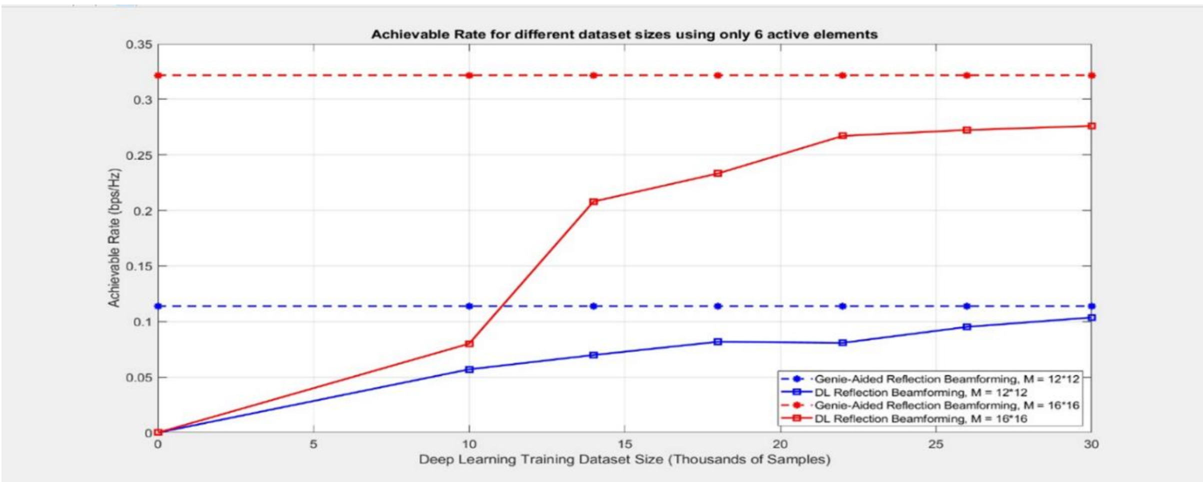

Figure 5.2 ANN MODEL OUTPUT GRAPH

Fig. 5.2 represents the achievable data rates for different data points using ANN model. This simulation is done for a RIS with 6 active elements. The x axis scales the number of data points and y axis scales the data rate. The dotted lines represent the maximum possible data rate and the normal line represents the data rate obtained by the ML model prediction. The blue colour lines are the results of 12*12 RIS and the red colour lines are the results of 16*16 RIS . As the size of data set increases the ML model accuracy increases. Around 30000 data points the predicted data rate gets close to the maximum achievable data rate. The above simulation is done for data set sizes of [5000,10000,15000,20000,25000,30000].

5.3. ALEXNET MODEL OUTPUT

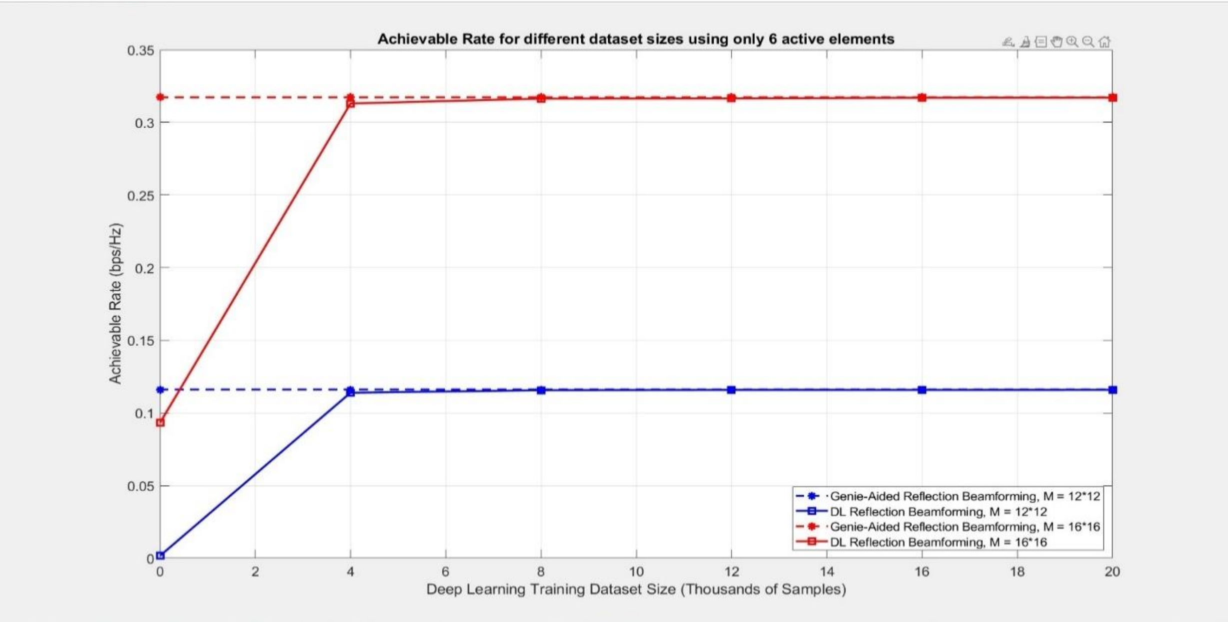

Figure 5.3 ALEXNET MODEL OUTPUT FOR DATASET SIZE 20000

Fig.5.3 shows the output plot of Alexnet model for data points [4000,8000,12000,16000,20000]. For the above data set size we get a predicted data rate output of [0.1139,0.1156,0.1158,0.1158,0.1159] for 12*12 RIS and [0.3130,0.3163,0.3165,0.3169,0.3169] for 16*16 RIS. We see that around 4000 data points the model is able to predict optimum data rate and after 4000 points the graph becomes a straight line reaching the maximum achievable data rate. So we run the simulation for data points of [1000,2000,3000,4000] and see an increasing plot.

Fig.5.4 shows the plot for data points up to 4000. Here we can see the accuracy increases as the data set size gets closer to 4000 and then overlaps with the maximum achievable data rate. For the above data set size we get a predicted data rate of [0.2701,0.2928,0.3152,0.3171] for 16*16 RIS and [0.1024,0.1105,0.1136,0.1145] for 12*12 RIS.

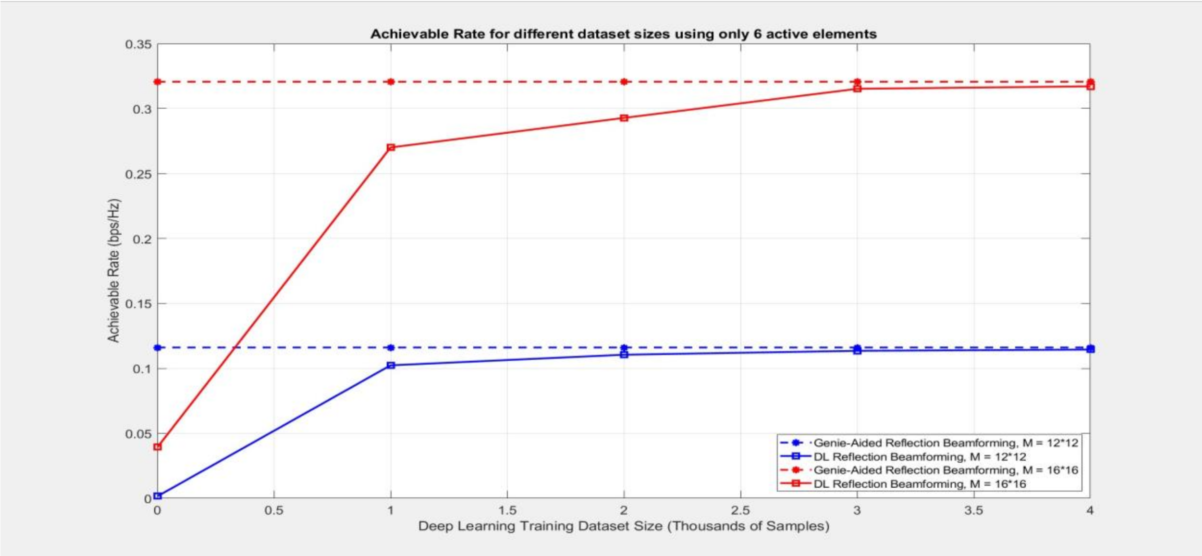

Figure 5.4 ALEXNET MODEL OUTPUT GRAPH

Fig.5.2 and fig.5.3 represents the achievable rate for various dataset sizes using ANN model and Alexnet model respectively. This simulation is done for a RIS with 6 active elements. The x axis scales the number of data points and y axis scales the data rate. The dotted lines represent the maximum possible data rate and the normal line represents the data rate obtained by the ML model prediction. The blue colour lines are the results of 12*12 RIS and the red colour lines are the results of 16*16 RIS.

In fig5.2 the model is trained with 30000 data points and still the predicted value does not match the maximum value. In fig5.3 at 4000 data points the predicted values are very close to the maximum possible values.

5.4 INFERENCE

We can see from the above plots the alexnet model is able to predict best beam forming vector to get maximum data rate at 4000 data points compared to the ANN model which takes more than 30000 data points to predict optimum data rate.

CHAPTER 6
CONCLUSION

This project is centred around developing an effective method for forecasting interaction matrices in RIS-assisted wireless communication systems. The goal is to create independent RIS architectures. By utilising advanced deep reinforcement learning frameworks, our proposed solution empowers the RIS to independently acquire and forecast the most effective RIS configurations by directly analysing sampling channel knowledge. Significantly, this approach obviates the requirement for an initial phase of gathering a dataset, setting it apart from solutions based on supervised learning. The simulation results, using precise ray-tracing channels, show that our technique achieves convergence at data rates close to optimum, with low beam training overhead and a restricted number of active elements. The utilisation of an AlexNet model demonstrates the efficiency of our method, attaining optimal data rates with only 4000 data samples, in contrast to an ANN model which necessitates 30000 data points to approximate the maximum data rate. This highlights the effectiveness and high performance of our suggested deep reinforcement learning technique in optimising RIS functionality for improved wireless communication systems.

6.1 FUTURE WORKS

A detailed model analysis and accuracy of the machine learning model developed in this project and the performance metrics analysis for the same shall be done. The maximum achievable data rate can be increased by increasing the bandwidth of the system since bandwidth is directly proportional to data rate. To do so the architecture of the channel should be modified and proper implementation of the above will result in a higher data for the RIS wireless link.

REFERENCES

[1] Baoling Sheen, Jin Yang, Xianglong Feng, and Md Moin Uddin Chowdhury, A Deep Learning Based Modelling of Reconfigurable Intelligent Surface Assisted Wireless Communications for Phase Shift Configuration. In IEEE Open Journal of the Communications Society, 2021

[2] Özgecan Özdogan, Emil Björnson, Deep Learning-based Phase Reconfiguration for Intelligent Reflecting Surfaces. In IEEE 54th Asilomar Conference on Signals, Systems, and Computers, 2020

[3] Abdelrahman Taha, Yu Zhang, Faris B. Mismar, Ahmed Alkhateeb, Deep Reinforcement Learning for Intelligent Reflecting Surfaces: Towards Standalone Operation. In IEEE International Workshop on Signal Processing Advances in Wireless Communications, 2020

[4] Mohammad Abrar, Md Habibur Rahman, Beom-Sik Shin, Ji-Hye Oh, Young-Hwan You, Hyoung-Kyu Song, Machine Learning for Intelligent-Reflecting-Surface-Based Wireless Communication towards 6G: A Review. In Sensors, 22(14), :2022

[5] Meng Xu, Shun Zhang, Caijun Zhong, Ordinary Differential Equation-Based CNN for Channel Extrapolation Over RIS-Assisted. In IEEE Communications Letters, 2021

[6] Ahmed Alkhateeb, DeepMIMO: A Generic Deep Learning Dataset for Millimeter Wave and Massive MIMO Applications. In Proc. of Information Theory and Applications Workshop, 2019

[7] S. V. Hum, J. Perruisseau-Carrier, Reconfigurable reflectarrays and array lenses for dynamic antenna beam control: A review, IEEE Trans. Antennas Propag., 2014.

[8] C. Huang, A. Zappone, G. C. Alexandropoulos, M. Debbah, and C. Yuen, ‘‘Reconfigurable intelligent surfaces for energy efficiency in wireless communication,’’ IEEE Trans. Wireless Commun., Aug. 2019

[9] C. Liaskos, S. Nie, A. Tsioliaridou, A. Pitsillides, S. Ioannidis, and I. Akyildiz, ‘‘A new wireless communication paradigm through software-controlled metasurfaces,’’ IEEE Commun. Mag., Sep. 2018.

[10] A. Alkhateeb, ‘‘DeepMIMO: A generic deep learning dataset for millimeter wave and massive MIMO applications,’’ in Proc. Inf. Theory Appl. Workshop (ITA), San Diego, CA, USA, Feb. 2019

[11] A. Faisal, H. Sarieddeen, H. Dahrouj, T. Y. Al-Naffouri, and M.-S. Alouini, ‘‘Ultra-massive MIMO systems at terahertz bands: Prospects and challenges,’’ 2019, arXiv:1902.11090

[12] E. Björnson, L. Sanguinetti, H. Wymeersch, J. Hoydis, and T. L. Marzetta, ‘‘Massive MIMO is a reality—What is next? Five promising research directions for antenna arrays,’’ 2019

[13] T. S. Rappaport, F. Gutierrez, E. Ben-Dor, J. N. Murdock, Y. Qiao, and J. I. Tamir, ‘‘Broadband millimeter-wave propagation measurements and models using adaptive-beam antennas for outdoor urban cellular communications,’’ IEEE Trans. Antennas Propag.,Apr. 2013.

[14] T. S. Rappaport, R. W. Heath Jr, R. C. Daniels, and J. N. Murdock, Millimeter Wave Wireless Communications. London, U.K.: Pearson, 2014.

[15] M. K. Samimi and T. S. Rappaport, ‘‘Ultra-wideband statistical channel model for non line of sight millimeter-wave urban channels,’’ in Proc. IEEE Global Commun. Conf., Dec. 2014

[16] S. Foo, ‘‘Liquid-crystal reconfigurable metasurface reflectors,’’ in Proc. IEEE Int. Symp. Antennas Propag. USNC/URSI Nat. Radio Sci. Meeting, Jul. 2017.

[17] Q. Wu and R. Zhang, ‘‘Intelligent reflecting surface enhanced wireless network via joint active and passive beamforming,’’ IEEE Trans. Wireless Commun., Nov. 2019.

[18] R. Mendez-Rial, C. Rusu, N. Gonzalez-Prelcic, A. Alkhateeb, and R. W. Heath, ‘‘Hybrid MIMO architectures for millimeter wave communications: Phase shifters or switches?’’ IEEE Access, vol. 4, 2016

[19] J. Lee, G.-T. Gil, and Y. H. Lee, ‘‘Exploiting spatial sparsity for estimating channels of hybrid MIMO systems in millimeter wave communications,’’ in Proc. IEEE Global Commun. Conf., Dec. 2014.

[20] Z. Tan, Y. C. Eldar, and A. Nehorai, ‘‘Direction of arrival estimation using co-prime arrays: A super resolution viewpoint,’’ IEEE Trans. Signal Process., Nov. 2014.